Journal of Materials Chemistry A

RSC Publishing

PAPER

View Article Online
View Journal | View Issue

Published on 02 September 2013. Downloaded by Fudan University on 17/03/2014 15:56:39.

Oriented PEDOT:PSS on aligned carbon nanotubes for efficient dye-sensitized solar cells†

Cite this: *J. Mater. Chem. A*, 2013, **1**, 13268

Guozhen Guan, Zhibin Yang, Longbin Qiu, Xuemei Sun, Zhitao Zhang, Jing Ren and Huisheng Peng*

Received 10th July 2013
Accepted 30th August 2013

DOI: 10.1039/c3ta12669b

www.rsc.org/MaterialsA

Aligned carbon nanotube–oriented poly(3,4-ethylenedioxythiophene):poly(styrene sulfonate) composites show an unexpectedly high catalytic activity which greatly exceeds the aligned individual components, the non-aligned composite counterpart, and even conventional platinum. When they are used as counter electrodes in dye-sensitized solar cells, the aligned composites also exhibit a highest energy conversion efficiency of 8.3%. The synergetic interaction between the nanotubes and polymers by aligned organization is the key to this new phenomenon.

Introduction

The orientation at the molecular and nanometer scales is key in controlling a material's structure and improving the material's properties.[1–3] Conjugated polymer molecules may be oriented by self-assembly during synthesis or by induction by external stimuli such as mechanical stretching and electric and magnetic fields after the synthesis.[4,5] However, the orientation mainly occurs in local regions and the degree of orientation is relatively low. On the other hand, the alignment of CNTs has been widely explored as a general and promising strategy to extend their remarkable mechanical and electronic properties from the nanoscale to the macroscopic scale.[6] Aligned CNT fibers exhibit high tensile strengths on the order of 10^3 MPa and electrical conductivities on the order of 10^3 S cm^{-1}, and are widely used for high performance structural materials and electronic devices.[7]

To improve the energy conversion efficiency of dye-sensitized solar cells (DSCs), it is critically important to develop high-performance electrode materials.[8] Due to their excellent electronic properties, carbon nanotubes (CNTs) and conducting polymers represent some of the most studied organic materials.[9–18] To further take advantage of their excellent properties, CNT–polymer composite materials have been widely studied in recent years.[19–23] However, the resulting DSCs showed much lower energy conversion efficiencies than expected as CNTs form a networked structure using the typical solution or melting methods. The charges have to transport through a lot of boundaries among CNT networks, with low efficiencies.[22] To this end, some attempts have been made to produce aligned CNT–polymer composites based on the use of aligned CNT arrays, sheets or fibers, though the polymer structure can not be effectively controlled.[23] In addition, the DSCs based on the aligned CNT–polymer composite film as the counter electrode exhibit lower energy conversion efficiencies compared with the conventional platinum electrode.[22]

To our best knowledge, herein we have developed, for the first time, aligned CNT–oriented polymer composite films by coating poly(3,4-ethylenedioxythiophene):poly(styrene sulfonate) (PEDOT:PSS) onto CNT sheets. This aligned composite film shows remarkable properties such as unexpectedly high electrocatalytic activity which greatly exceeds the bare aligned CNTs, bare oriented PEDOT:PSS, a randomly dispersed CNT–PEDOT:PSS composite, and even metals such as platinum. The synergetic interaction between the CNTs and polymer chains by aligned organization is the key to this new phenomenon. When the aligned composite film is used as a counter electrode in DSCs, it exhibits a maximum energy conversion efficiency of 8.3%, which is much higher than the bare aligned CNTs or PEDOT:PSS, a randomly dispersed CNT–PEDOT:PSS composite and conventional platinum.

Experimental section

The preparation of a single layer of an aligned CNT sheet with a thickness of appropriately 20 nm has been previously described,[24] and many layers of CNT sheets could be further stacked into thicker layers along the CNT-aligned direction. The aligned CNT–PEDOT:PSS composite films were prepared as follows. PEDOT:PSS solution (15 mg mL^{-1}) in a solvent mixture of water and *N*,*N*-dimethylformamide (volume ratio of 1 : 2) was spin-coated onto the aligned CNT sheets at 5000 revolutions per minute for 15 s. After evaporation of the solvents at room

State Key Laboratory of Molecular Engineering of Polymers, Department of Macromolecular Science, Laboratory of Advanced Materials, Fudan University, Shanghai 200438, China. E-mail: penghs@fudan.edu.cn

† Electronic supplementary information (ESI) available. See DOI: 10.1039/c3ta12669b

This journal is © The Royal Society of Chemistry 2013

Published on 02 September 2013. Downloaded by Fudan University on 17/03/2014 15:56:39.

temperature, the composite films were annealed at 140 °C for 30 min in argon. The length and width of the CNT sheets for DSCs were both 6 mm. The oriented PEDOT:PSS films were prepared by shearing PEDOT:PSS solution onto the substrates unidirectionally through a doctor-blading process. After evaporation of the solvent at room temperature, the films were annealed at 140 °C for 30 min in argon.

To fabricate the DSCs, TiO_2 nanoparticles composed of a layer of nanocrystalline TiO_2 (diameter of 20 nm) with a thickness of 14 μm and a light-scattering layer of TiO_2 (diameter of 200 nm) with a thickness of 2 μm were deposited onto the FTO glass by a screen printing technique and dried at 120 °C for 5 min. The resulting film was further heated to 500 °C for 30 min. After cooling to room temperature, it was immersed into an aqueous solution of $TiCl_4$ (40 mM) at 70 °C for 30 min and rinsed with deionized water, followed by sintering at 500 °C for 30 min. After cooling down to 120 °C, the electrode was immersed into a 0.3 mM solution of the N719 dye in a mixture of acetonitrile and *tert*-butanol (volume ratio of 1 : 1) for 16 h. The dye-absorbed working electrode was assembled with the counter electrode by a Surlyn frame with a thickness of 25 μm as the spacer at a pressure of 0.2 MPa and a temperature of 125 °C. The electrolyte containing 0.1 M lithium iodide, 0.05 M iodine, 0.6 M 1,2-dimethyl-3-propylimidazolium iodide and 0.5 M 4-*tert*-butyl-pyridine was injected through a hole in the counter electrode. The hole was finally sealed by Surlyn and a cover slide. In the case of flexible DSCs, a suspension of TiO_2 particles in ethanol (20 wt%) was coated onto a flexible conducting substrate by a doctor-blading method. After it was dried at 120 °C for 30 min, the working electrode was immersed in the N719 solution to fabricate the flexible DSCs.

Scanning electron microscopy was performed on a Hitachi FE-SEM S-4800 instrument operated at 1 kV. Polarized UV-vis spectra were collected on a SHIMADZU UV-2550 instrument with a GLB5-UV polarizer from Thorlabs. Raman spectra were obtained from a Renishaw inVia Raman microscope with an excitation wavelength of 632.8 nm. Polarized Raman spectra were collected using polarized light (wavelength of 632.8 nm) with a rotation mount PRM05GL5 from Thorlabs. The film thickness was measured by a Dektak 150 Step Profiler. The *J–V* curves of the DSCs were recorded by a Keithley 2400 Source Meter under the illumination (100 mW cm^{-2}) of simulated AM1.5 solar light from a solar simulator (Oriel-Sol3A 94023A equipped with a 450 W Xe lamp and an AM1.5 filter). The light intensity was calibrated using a reference Si solar cell (Oriel-91150). An electrochemical analyzer (Shanghai Chenhua CHI 660D) was used to obtain the cyclic voltammograms (in an acetonitrile solution containing I_2, LiI and $LiClO_4$), Nyquist plots and Tafel curves.[16]

Results and discussion

To prepare the composite film, aligned CNT sheets were firstly pulled out of CNT arrays synthesized by chemical vapor deposition, according to our previous reports.[5,8] The synthesized CNTs feature a multi-walled structure with a diameter of ~10 nm (Fig. S1†). A PEDOT:PSS solution was then spin-coated onto the CNT sheet to form a high quality composite film. Fig. 1a and b show scanning electron microscopy (SEM) images of a typical, uniform composite film where the CNTs remain highly aligned with each other.

Raman spectroscopy can be used to investigate composite films.[25] Fig. 1c compares the Raman spectrum of the composite film with the bare aligned CNT sheets and PEDOT:PSS. The D*, G, and D modes of the CNTs at 2654, 1583 and 1329 cm^{-1} in the aligned CNT sheet are shifted to 2652, 1586 and 1335 cm^{-1} after the incorporation of PEDOT:PSS, respectively. The red shift in the D* mode indicates the decreasing energy band gap of π electrons within the CNT–PEDOT:PSS interactions, which increases the charge transfer efficiency among the aligned CNTs.[26–28] In contrast, the blue shift of the other modes shows that the intermolecular interaction between CNT and PEDOT:PSS enhances the phonon excitation energy with the increasing coherence length and electron mobility under the electron–phonon scattering and binding.[29,30] Meanwhile, the conjugated aromatic ring modes of oriented PEDOT:PSS at 1427 and 988 cm^{-1} shift to 1431 and 990 cm^{-1} respectively after the formation of the composite films. These phenomena verify the strong interactions between the CNTs and the conjugated thiophene chain.[31]

The orientation of the PEDOT:PSS chains in the composite film can be evaluated by both polarized Raman and UV spectroscopy.[32] The Raman signals are produced by both CNTs and PEDOT:PSS, while the UV signals are obtained by subtracting the absorption of the CNTs. The polarized and aligned directions of the CNTs and the included angle are shown schematically in Fig. 2a. Obviously, the intensity of the characteristic peak at 1430 cm^{-1} for PEDOT in the polarized Raman spectrum increases with the increase of the included angle from 0 to 90° (Fig. 2b), which indicates the orientation of the PEDOT chains. As the $C_\alpha{=}C_\beta(-O)$ stretch of the thiophene ring is perpendicular to the PEDOT backbone,[31] the orientation of the PEDOT backbone is parallel with the CNT-aligned direction. Meanwhile, the intensity of the characteristic peak at 227 nm for the PSS in the polarized UV spectrum decreases as the included angle increases from 0 to 90° (Fig. 2c). The dichroic ratio, R_{UV} ($R = I_{\parallel}/I_{\perp}$, where $I_{\parallel}$ and $I_{\perp}$ correspond to the intensities of the characteristic peak at parallel and perpendicular directions relative to the CNT-aligned direction, respectively), is obtained to be 3.3. The orientation coefficient *f* is then calculated from the dichroic ratio (*R*) using $f = (R - 1)/(R + 2)$, *i.e.*, $f_{UV} = 0.43$. Therefore, the polymer backbones should be oriented along the CNT length,[19,20] with aromatic rings exposed to the surface, which are expected to offer catalytic activity.[33,34]

Cyclic voltammetry (CV) was used to investigate the catalytic activity of the aligned composite film.[35,36] To this end, bare aligned CNT sheets, bare oriented PEDOT:PSS (Fig. S2†), randomly dispersed CNT–PEDOT:PSS composite film and platinum were studied for comparison (Fig. 3a). Neither the aligned CNT sheet nor PEDOT:PSS showed two pairs of oxidation–reduction peaks in the I^-/I_3^- electrolyte, and they exhibited much lower catalytic activity than the platinum

Published on 02 September 2013. Downloaded by Fudan University on 17/03/2014 15:56:39.

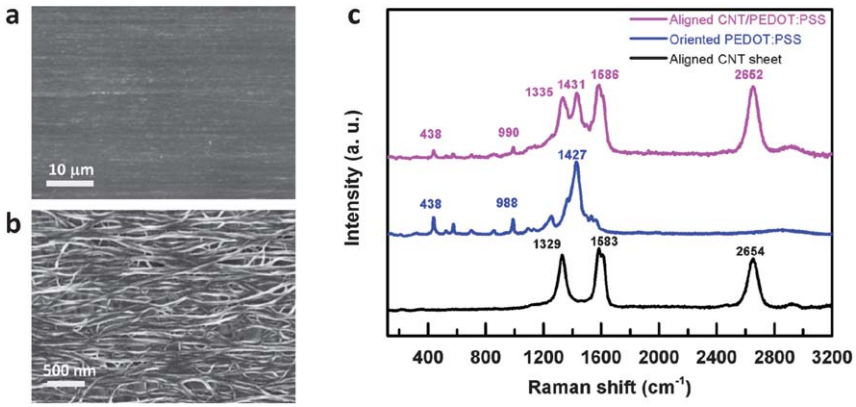

Fig. 1 Characterization of the aligned CNT–PEDOT:PSS composite. (a and b) Scanning electron microscopy (SEM) images of the composite at low and high magnifications, respectively. (c) Raman spectra of aligned CNT sheets, oriented PEDOT:PSS, and the aligned CNT–PEDOT:PSS composite.

electrode. The two pairs of peaks can be clearly observed for both the aligned and randomly dispersed CNT–PEDOT:PSS composite films. Generally, a higher reduction peak current density (I_p) or a lower peak-to-peak voltage separation (V_{PP}) indicates a higher catalytic activity.[37] Here the V_{PP} value of the aligned CNT–PEDOT:PSS film is 0.38 V, which is much lower than 0.67 V for the randomly dispersed CNT composite, and even lower than 0.47 V for conventional platinum. In the randomly dispersed CNT composite, the electrophilic PEDOT backbones are wrapped by nucleophilic PSS chains, so the aromatic ring catalytic sites are not exposed to the electrolyte.[28,33] In addition, the many boundaries among the randomly dispersed CNTs decrease the charge separation and transport due to the high contact resistance.[36] In contrast, the PEDOT:PSS chains are highly oriented by the aligned CNTs with catalytic sites effectively exposed to the electrolyte, and the charges can be also rapidly transported along the aligned CNTs.[24] Here the aligned CNT–PEDOT:PSS composite film also exceeds platinum in catalytic activity due to the much higher surface area enabled by the aligned nanostructure.

The aligned CNT–PEDOT:PSS composite films may represent a new family of electrode materials, and here they have been used as counter electrodes to fabricate DSCs. A series of composite films which are prepared from the same CNT sheet (40 nm in thickness) but coated with increasing weight percentages of PEDOT:PSS are compared (Fig. S3 and Table S1†). With the increasing polymer weight percentage, the open-circuit photovoltage (V_{OC}) remains almost unchanged while both the short circuit current density (J_{SC}) and fill factor (FF) are first increased and then decreased. The optimal polymer weight percentage occurs at approximately 33%.

Fig. 3b compares the *J–V* curves of DSCs with the aligned CNT–PEDOT:PSS composite (with a polymer weight percentage of 33%), randomly dispersed CNT–PEDOT:PSS composite (with a polymer weight percentage of 33%), aligned CNT sheet, oriented PEDOT:PSS and platinum as the counter electrodes measured under AM1.5 illumination, and the detailed photovoltaic parameters are further summarized in Table 1. The V_{OC} of the five DSCs are almost the same at ~0.72 V, while the J_{SC} and FF are largely varied due to the different performances of the counter electrodes. For the oriented PEDOT:PSS electrode, the resulting DSC shows a J_{SC} of 14.5 mA cm^{-2} and FF of 0.33 with a maximum energy conversion efficiency (η) of 3.4%. For the bare aligned CNT sheet, the resulting DSC exhibits a J_{SC} of 13.5 mA cm^{-2} and FF of 0.50 with a maximum η of 5.0%. After the combination of the aligned CNTs and PEDOT:PSS, the J_{SC} and FF increased to 16.1 mA cm^{-2} and 0.71 respectively to produce a η of 8.3%. As a comparison, the randomly dispersed CNT–PEDOT:PSS composite showed a much lower efficiency of 4.0%, and the platinum electrode produces an efficiency of 7.5%. To summarize, the energy conversion efficiency based on the aligned CNT–PEDOT:PSS composite film is appropriately 2.1 times that of the randomly dispersed CNT–PEDOT:PSS composite, 1.7 times that of the aligned CNT sheet, 2.4 times that of the oriented PEDOT:PSS, and 1.1 times that of the platinum electrode.

To further investigate the promising applications of aligned CNT–PEDOT:PSS composite films, electrochemical impedance spectroscopy was used to compare the above DSCs (Fig. 3c).[16,37] The spectrum typically shows two semicircles, with the first semicircle used to evaluate the catalytic properties of the counter electrode. The smaller first semicircle shows a decrease in the series resistance, which leads to an increase the FF, giving a higher energy conversion efficiency. Obviously, the aligned CNT–PEDOT:PSS composite film has a much lower series resistance than the bare aligned CNT and oriented PEDOT:PSS films. In addition, for the first semicircle, the series resistance of the aligned CNT–PEDOT:PSS composite is 1/7 that of the randomly dispersed CNT–PEDOT:PSS composite and 1/2 that of the platinum. The second semicircle corresponds to the charge transfer at the TiO_2/dye/electrode interface in the middle-frequency region. The aligned CNT–PEDOT:PSS composite also has a smaller size than the randomly dispersed CNT–PEDOT:PSS composite, bare aligned CNTs, oriented PEDOT:PSS and platinum.

 This journal is © The Royal Society of Chemistry 2013

Published on 02 September 2013. Downloaded by Fudan University on 17/03/2014 15:56:39.

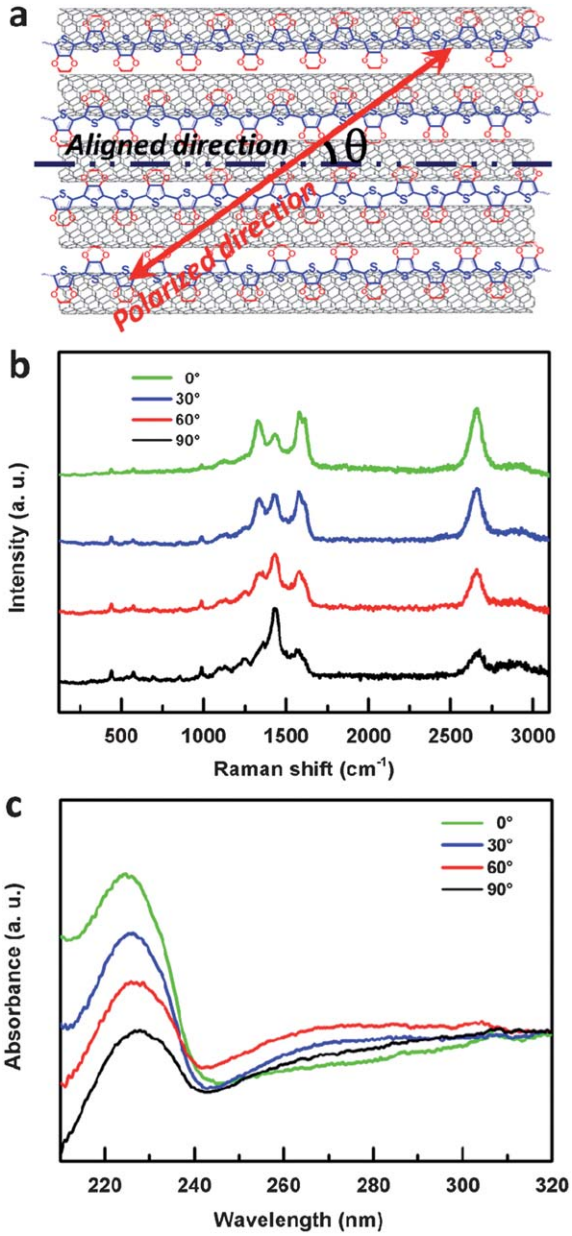

Fig. 2 Oriented PEDOT:PSS on aligned CNTs. (a) Schematic illustration of the included angle (θ) between the polarized and CNT-aligned directions. (b and c) Polarized Raman ultraviolet spectra of the aligned CNT–PEDOT:PSS composite for the included angles of 0°, 30°, 60°, and 90°.

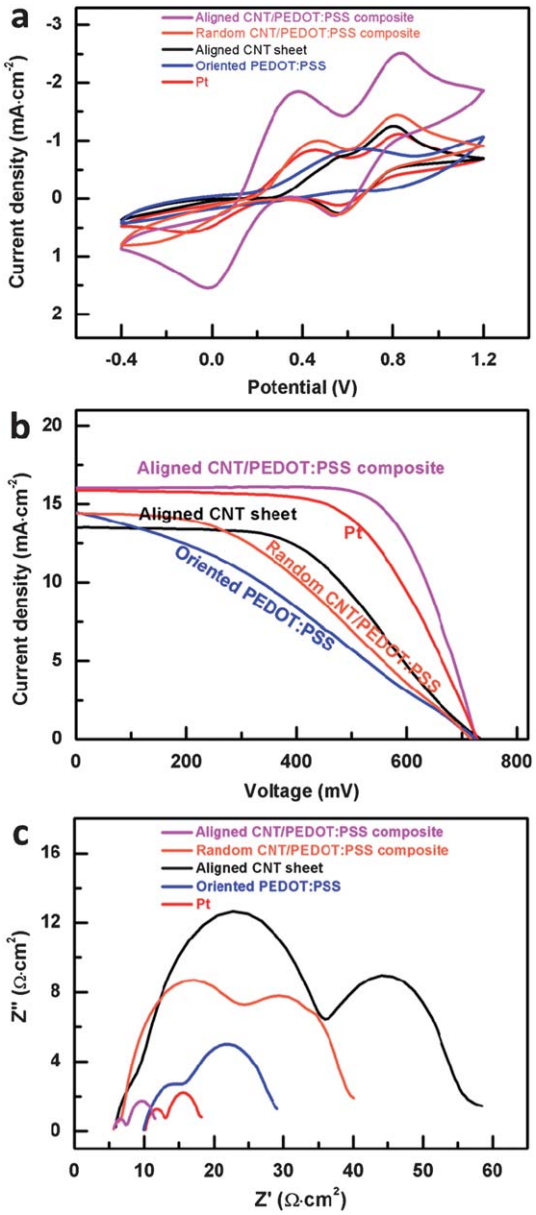

Fig. 3 Comparison of the platinum, aligned CNT sheet, oriented PEDOT:PSS, randomly dispersed CNT–PEDOT:PSS and aligned CNT–PEDOT:PSS composite (with the polymer weight percentage of 33%) materials as the counter electrodes in DSCs. (a) Cyclic voltammograms. (b) *J*–*V* curves. (c) Nyquist plots.

The electrochemical catalytic activity of the different counter electrodes were also compared by EIS and Tafel polarization measurements, which were carried out in a symmetrical dummy cell fabricated with two counter electrodes and using the same electrolyte as in the DSCs.[14,16] The curves are shown in Fig. S4 and S5† and further summarized in Table S2.† The aligned CNT–PEDOT:PSS composite and platinum exhibited excellent electrochemical catalytic activity. In addition, the aligned CNT–PEDOT:PSS composite showed the lowest charge transfer resistance of 1.6 Ω cm^2 and the highest exchange current density of 7.8 mA cm^{-2}. The exchange current densities were confirmed by the Tafel curves. The dummy cells

Table 1 Photovoltaic parameters of the DSCs based on the different counter electrodes in Fig. 3b

Counter electrode	V_{OC} (V)	J_{SC} (mA cm^{-2})	FF	η (%)
Aligned CNT–PEDOT:PSS	0.731	16.1	0.71	8.3
Random CNT–PEDOT:PSS	0.720	14.4	0.39	4.0
Oriented PEDOT:PSS	0.723	14.5	0.33	3.4
Aligned CNT sheet	0.733	13.5	0.50	5.0
Pt	0.728	16.2	0.64	7.5

Published on 02 September 2013. Downloaded by Fudan University on 17/03/2014 15:56:39.

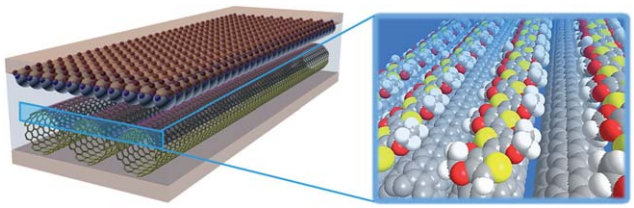

Fig. 4 Schematic illustration of the oriented PEDOT:PSS on aligned CNTs for efficient DSCs. The grey, white, yellow and red colors correspond to elements C, H, S and O , respectively.

demonstrated the same rule on the variation of exchange current densities as the DSCs.

A series of aligned CNT–PEDOT:PSS composite films, which are prepared by coating the same concentration of PEDOT:PSS solution onto CNT sheets of increasing thickness (*i.e.*, 40 nm, 200 nm, 1 μm, and 2 μm) and the same width and length, were also compared (Fig. 3b, S6–S8 and Table S3†). The composite films with sheet thicknesses of 2 μm after the coating of PEDOT:PSS correspond to the polymer weight percentage of 33%. Both the V_{OC} and J_{SC} are not significantly changed, but the FF increases significantly with the increasing thickness of the CNT sheets or the decreasing polymer weight percentage. The energy conversion efficiencies are therefore continuously enhanced from 5.1, 5.8, 7.4 to 8.3%, respectively, which has been verified by cyclic voltammetry (Fig. S9†). With further increasing the thickness of the CNT sheet to 4 μm, the efficiency remains almost unchanged at 8.39% (Fig. S10†).

The PEDOT:PSS film has been widely studied for photovoltaic devices due to its high ductility. As expected, these CNT–PEDOT:PSS composite films are also shown to be highly flexible with high transmittances (Fig. S11†). The aligned structure of the CNTs in Fig. 1a and b can be maintained well, according to SEM observations, when the composite film is bent into different forms. The high flexibility of the composite film was further quantitatively verified by tracing the electrical resistance during the deformation. The composite resistances varied slightly, by less than 1%, in 2000 cycles (Fig. S12†). The composite film can be widely used to fabricate flexible and efficient devices compared with rigid metal electrodes and silicon-based technologies. As a demonstration of their applications, the composite films are also successfully used to make flexible DSCs (Fig. S13†).

Conclusion

In summary, aligned CNT sheets are found to effectively induce the orientation of conjugated PEDOT:PSS complex chains by π–π interactions. Unexpectedly, the synergetic interaction between the CNTs and PEDOT:PSS chains through the aligned structure offers much higher catalytic activity than the bare aligned CNT sheet, bare oriented PEDOT:PSS, randomly dispersed CNT–PEDOT:PSS, and even conventional platinum. When they are used as electrodes to fabricate DSCs (Fig. 4), the aligned CNT–PEDOT:PSS composite produces the highest maximum energy conversion efficiency of 8.3%. This work also represents a general and effective paradigm in the development of high performance composite materials for efficient opto-electronic and electronic devices.

Acknowledgements

This work was supported by NSFC (91027025, 21225417), MOST (2011CB932503, 2011DFA51330), STCSM (11520701400, 12nm0503200), Fok Ying Tong Education Foundation and The Program for Professor of Special Appointment at Shanghai Institutions of Higher Learning.

References

1 G. F. Zou, H. M. Luo, S. Baily, Y. Y. Zhang, N. F. Haberkorn, J. Xiong, E. Bauer, T. M. McCleskey, A. K. Burrell, L. Civale, Y. T. Zhu, J. L. MacManus-Driscoll and Q. X. Jia, *Nat. Commun.*, 2011, **2**, 428.
2 Y.-K. Kim, B. Senyuk and O. D. Lavrentovich, *Nat. Commun.*, 2012, **3**, 1133.
3 Y. Kim, S. Cook, S. M. Tuladhar, S. A. Choulis, J. Nelson, J. R. Durrant, D. D. C. Bradley, M. Giles, I. McCulloch, C.-S. Ha and M. Ree, *Nat. Mater.*, 2006, **5**, 197.
4 W. Makiguchi, S. Kobayashi, Y. Furusho and E. Yashima, *Angew. Chem., Int. Ed.*, 2013, **52**, 5275.
5 R. Joseph Kline, M. D. McGehee and M. F. Toney, *Nat. Mater.*, 2006, **5**, 222.
6 X. Sun, T. Chen, Z. Yang and H. Peng, *Acc. Chem. Res.*, 2013, **46**, 539.
7 H. Peng, *J. Am. Chem. Soc.*, 2008, **130**, 42.
8 T. Chen, L. Qiu, Z. Yang and H. Peng, *Chem. Soc. Rev.*, 2013, **42**, 5031.
9 G. Li, F. Wang, Q. Jiang, X. Gao and P. Shen, *Angew. Chem., Int. Ed.*, 2010, **49**, 3653.
10 L. Hu, D. S. Hecht and G. Grüner, *Chem. Rev.*, 2010, **110**, 5790.
11 C. J. Brabec, S. Gowrisanker, J. J. M. Halls, D. Laird, S. Jia and S. P. Williams, *Adv. Mater.*, 2010, **22**, 3839.
12 F. Cheng, J. Liang, Z. Tao and J. Chen, *Adv. Mater.*, 2011, **23**, 1695.
13 B. Fan, X. Mei, K. Sun and J. Ouyang, *Appl. Phys. Lett.*, 2008, **93**, 143103.
14 G. Yue, J. Wu, Y. Xiao, J. Lin, M. Huang, Z. Lan and L. Fan, *Energy*, 2013, **54**, 315.
15 S. Mazzucchelli, M. Colombo, P. Verderio, E. Rozek, F. Andreata, E. Galbiati, P. Tortora, F. Corsi and D. Prosperi, *Angew. Chem., Int. Ed.*, 2013, **52**, 3121.
16 Z. Lan, J. Wu, J. Lin and M. Huang, *J. Mater. Chem.*, 2012, **22**, 3948.
17 X. Mei, S. J. Cho, B. Fan and J. Ouyang, *Nanotechnology*, 2010, **21**, 395202.
18 Q. Li, J. Wu, Q. Tang, Z. Lan, P. Li, J. Lin and L. Fan, *Electrochem. Commun.*, 2008, **10**, 1299.
19 H. Peng, X. Sun, F. Cai, X. Chen, Y. Zhu, G. Liao, D. Chen, Q. Li, Y. Lu, Y. Zhu and Q. Jia, *Nat. Nanotechnol.*, 2009, **4**, 738.

 This journal is © The Royal Society of Chemistry 2013

Published on 02 September 2013. Downloaded by Fudan University on 17/03/2014 15:56:39.

20 X. Sun, W. Wang, L. Qiu, W. Guo, Y. Yu and H. Peng, *Angew. Chem., Int. Ed.*, 2012, **51**, 8520.
21 D. R. Kauffman and A. Star, *Angew. Chem., Int. Ed.*, 2008, **47**, 6550.
22 S. Huang, L. Li, Z. Yang, L. Zhang, H. Saiyin, T. Chen and H. Peng, *Adv. Mater.*, 2011, **23**, 4707.
23 X. Sun, T. Chen, Z. Yang and H. Peng, *Acc. Chem. Res.*, 2013, **46**, 539.
24 Z. Yang, T. Chen, R. He, G. Guan, H. Li, L. Qiu and H. Peng, *Adv. Mater.*, 2011, **23**, 5436.
25 G. Guan, Z. Qiu, X. Sun, Z. Yang, L. Qiu, Q. Ma and H. Peng, *J. Mater. Chem.*, 2012, **22**, 18653.
26 M. Gratzel, *Acc. Chem. Res.*, 2009, **42**, 1788.
27 G. Li, F. Wang, Q. Jiang, X. Gao and P. Shen, *Angew. Chem., Int. Ed.*, 2010, **49**, 3653.
28 D.-J. Yun, K. Hong, S. h. Kim, W.-M. Yun, J.-Y. Jang, W.-S. Kwon, C.-E. Park and S.-W. Rhee, *ACS Appl. Mater. Interfaces*, 2011, **3**, 43.
29 S. Bhandari, M. Deepa, A. K. Srivastava, A. G. Joshi and R. Kant, *J. Phys. Chem. B*, 2009, **113**, 9416.
30 V. Perebeinos, J. Tersoff and P. Avouris, *Phys. Rev. Lett.*, 2005, **94**, 086802.
31 B. Winther-Jensen and K. West, *Macromolecules*, 2004, **37**, 4538.
32 W. Wang, X. Sun, W. Wu, H. Peng and Y. Yu, *Angew. Chem., Int. Ed.*, 2012, **51**, 4644.
33 H. Hopf and M. S. Sherburn, *Angew. Chem., Int. Ed.*, 2012, **51**, 2298.
34 Z. Lin and X. Wang, *Angew. Chem., Int. Ed.*, 2013, **52**, 1735.
35 Y. Xue, J. Liu, H. Chen, R. Wang, D. Li, J. Qu and L. Dai, *Angew. Chem., Int. Ed.*, 2012, **51**, 12124.
36 Z. Yang, M. Liu, C. Zhang, W. W. Tjiu, T. Liu and H. Peng, *Angew. Chem., Int. Ed.*, 2013, **52**, 3996.
37 J. Halme, P. Vahermaa, K. Miettunen and P. Lund, *Adv. Mater.*, 2010, **22**, E210.